Scientific Research Publishing

Open Journal of Geology, 2023, 13, 431-448
https://www.scirp.org/journal/ojg
ISSN Online: 2161-7589
ISSN Print: 2161-7570

Study on the LAI Single Tree Model Based on Terrestrial Laser Scanning

Zhaohua Pan[1], Genshen Fu[2*]

[1]Hefei 168 High School, Hefei, China
[2]School of Forestry and Landscape Architecture, Anhui Agricultural University, Hefei, China
Email: *fugenshen2021@163.com

How to cite this paper: Pan, Z.H. and Fu, G.S. (2023) Study on the LAI Single Tree Model Based on Terrestrial Laser Scanning. *Open Journal of Geology*, **13**, 431-448.
https://doi.org/10.4236/ojg.2023.135020

Received: March 28, 2023
Accepted: May 28, 2023
Published: May 31, 2023

Abstract

Leaf area index (LAI) is a key parameter for studying global terrestrial ecology and environment and has great ecological significance. How to accurately measure and calculate structural parameters of trees has become an urgent matter. This paper reports the use of terrestrial laser scanning (TLS) as a measurement tool to achieve accurate LAI estimation through point cloud preprocessing measures, the LeWos algorithm, and voxel methods. The accuracy and feasibility of this indirect measurement method were explored. It is found that the single wood structure parameters extracted from TLS have a good linear relationship with manual measurement, and the extraction errors meet the requirements of real-scene conversion. The study also found when the voxel size is consistent with the minimum distance of the point cloud set by TLS instrument, it has a strong correlation with the measured value of canopy analyser. These results lay the foundation for conveniently and quickly obtaining structural parameters of trees, tree growth state detection, and canopy ecological benefit assessment.

Keywords

Leaf Area Index, Terrestrial Laser Scanning, Branch-Leaf Separation, Point Cloud Voxelization

1. Introduction

Plant canopy is an important part of terrestrial ecosystem between atmosphere and soil matrix for organic matter synthesis and metabolism, which plays an important role in maintaining the balance of carbon and oxygen and the sustainable development of human society [1]. Canopy structure further reveals the intrinsic genetic characteristics of plants and the role of the external environ-

ment, and is closely related to natural phenomena such as light energy transmission, rainwater interception, transpiration loss, and ground temperature regulation [2] [3] [4]. Leaf area index (LAI), as an important quantitative index to describe structure of plant canopy, is equivalent to structural characteristics and ecological significance of plant canopy, and has become a key parameter in study of global terrestrial ecology and environmental response [5].

LAI was initially used to quantitatively describe leaf growth and density changes at plant population level, but its connotation has also changed with the deepening of measurement methods and application levels [6]. At present, the mainstream definition is Chen's "total unilateral area of leaf tissue per unit of ground surface area (m^2/m^2)" [7]. Over the years, the research and overview of LAI measurement methods can be summarized as direct measurement and indirect measurement. Direct measurement is usually in strict accordance with the definition of LAI, generally requires destructive sampling, and even whole plant harvest. Common methods include punching weighing method, grid method, pattern weighing method, etc. [8]. However, the whole process of direct measurement is complex, time-consuming and labor-intensive, and is not suitable for large-area measurement, especially for tall trees. Indirect measurement is to derive LAI by using coupling relationship between plant canopy structure and surrounding radiation environment. The theory involves many parameters such as Beer-Lambert law, aggregation effect, zenith angle, azimuth angle and transmittance [9] [10] [11]. The biggest advantage of indirect measurement is that it does not affect the normal growth and development of plants, and the access is convenient and quick. Optical sensors are widely used in indirect measurement methods. The commonly used instruments are LAI-2200 canopy analyzer, fisheye camera, etc. [12]. However, traditional optical sensor has light saturation effect, which is easy to underestimate high LAI value. The main reason is that traditional optical sensor obtains two-dimensional information and lacks more vertical structure information inside canopy [13] [14] [15]. Compared with the limitations of traditional optical sensors, the emerging laser radar technology is increasingly favored by scholars. It can obtain fine three-dimensional information of ground objects, retain vertical structure of canopy to the greatest extent, and effectively weaken light saturation limit. It has been widely used in the estimation of leaf area index [16] [17].

Light detection and ranging (LiDAR), is an active remote sensing technology, which rapidly obtains 3D spatial information of ground objects through transmitting and receiving laser signals and is reflected in computers in the form of "point cloud" (*i.e.* the collection of laser reflection points of ground objects' surface profiles) [18]. According to the sensor platform, it can be divided into ground, airborne and space-borne laser scanning technologies [19]. Generally, airborne and space-borne platforms have certain limitations in point cloud resolution and acquisition of horizontal and vertical structure information inside canopy. In order to be applicable to large-scale LAI estimation, a large amount of ground data is needed for verification and correction [20] [21] [22]. Terrestri-

al laser scanning (TLS) has higher measurement accuracy, which can accurately construct tree crown structure through massive point clouds and reflect more depth information [23]. Common methods used to estimate LAI in TLS include hemispherical projection method and stereo pixel method. Hemispherical projection method is to project point clouds onto hemispherical surfaces by means of spheroidal plane projection or Lambert azimuth equal-area projection, then calculate porosity in two-dimensional planes, and finally deduce effective LAI [24]. The three-dimensional pixel method (*i.e.* the voxel method) divides point clouds according to the voxel grid and determines whether point clouds fall into the grid to calculate leaf area density (LAD). Finally, the LAI value is obtained by accumulating the LAD of each layer with vertical height [25]. Later, convex hull algorithm and echo conversion method were derived. These methods basically optimized the estimation of different parameters as much as possible on the original basis, and constantly improved the estimation of LAI [26] [27]. All these methods above indicate that LiDAR technique has three-dimensional advantages and far-reaching prospects for LAI inversion to varying degrees.

At present, it is a generally accepted way to indirectly derive real LAI by using voxels to retain characteristics of real canopy structure. However, there are also problems of optimal voxel size and branch point cloud being included in the process, which affects the estimation accuracy of LAI. Wood components such as branches are often neglected in previous accurate calculation of LAI. Therefore, this paper obtains a complete single tree point clouds through a variety of preprocessing methods, and then uses the LeWos algorithm to separate branch and leaf point clouds. Finally, a LAI voxel model that removes the wood components and only includes the leaf point cloud is constructed to achieve accurate estimation of canopy LAI. The research results can provide a basis for large-scale LAI estimation using LiDAR sensors carried by drones or satellites, and further provide research ideas for monitoring the growth status of trees and evaluating the ecological benefits of canopy.

2. Materials and Methods

2.1. Sample Wood Setting

The research site of this experiment was selected in the campus of Anhui Agricultural University. Through field investigation, 10 landscaping tree species were selected, and 20 plants were sampled (**Table 1**). In order to accurately obtain a three-dimensional model of a single tree with complete structure, individual trees with no public facilities shelter near the ground and no obvious overlapping of adjacent canopy branches and leaves are preferred.

2.2. TLS Data Acquisition and Preprocessing

2.2.1. TLS Setup and Target Sphere Placement

The basic data required for this experiment were collected using TLS of Zhonghaida HS450. The device can sensitively calculate time difference between pulse

Table 1. Species and amounts of trees.

No.	Species	Amounts
1	*Koelreuteria paniculata* Laxm.	2
2	*Cinnamomum camphora* (L.) J. Presl	2
3	*Ligustrum lucidum* W. T. Aiton	2
4	*Albizia julibrissin* Durazz.	2
5	*Firmiana simplex* (L.) W. Wight	2
6	*Metasequoia glyptostroboides* Hu & W. C. Cheng	1
7	*Pinus massoniana* Lamb.	3
8	*Magnolia grandiflora* L.	3
9	*Platanus acerifolia* (Aiton) Willdenow.	2
10	*Sapindus saponaria* L.	1

laser from the emission position to contact surface and then back to the receiver, and obtain the high-precision XYZ relative spatial coordinates of the contact point on outer surface of the object. It can complete the three-dimensional imaging with a horizontal perspective of 360˚ and a vertical perspective of 100˚. In order to fully collect the global details of the external contour of a single tree, three-station erection or multi-station erection method is used to carry out three-dimensional scanning operations around different directions of the same target. At the same time, in order to accurately splice multi-station point cloud data, it is necessary to evenly place multiple target balls with bright reflection surfaces in public field of view between stations, which can be used as a highlight overlap mark (*i.e.*, constructing homonymous points) for fine stitching of each station image.

2.2.2. TLS Data Preprocessing

The original point cloud data of TLS need to go through the preprocessing steps of point cloud splicing, filtering and segmentation in turn, and then obtain the complete structural point cloud used to extract the DBH, crown width, tree height, first branch height and canopy volume parameters of single tree. The TLS processing scenario is shown in **Figure 1**.

Point cloud stitching, that is, point cloud registration, is to find the spatial transformation relationship between the point sets of each station in different coordinate systems to match the homonymous points, so that the point sets of each station are unified into the same coordinate system, and the point clouds of the intersecting areas are completely overlapped. We use the iterative closest point (ICP) fine registration algorithm, which is based on the least square method. The rotation and translation parameters of the optimal rigid body transformation are iteratively calculated according to the relationship point pairs generated by the matching of the homonymous point markers until they converge to the millimeter-level accuracy requirement of complete registration [28].

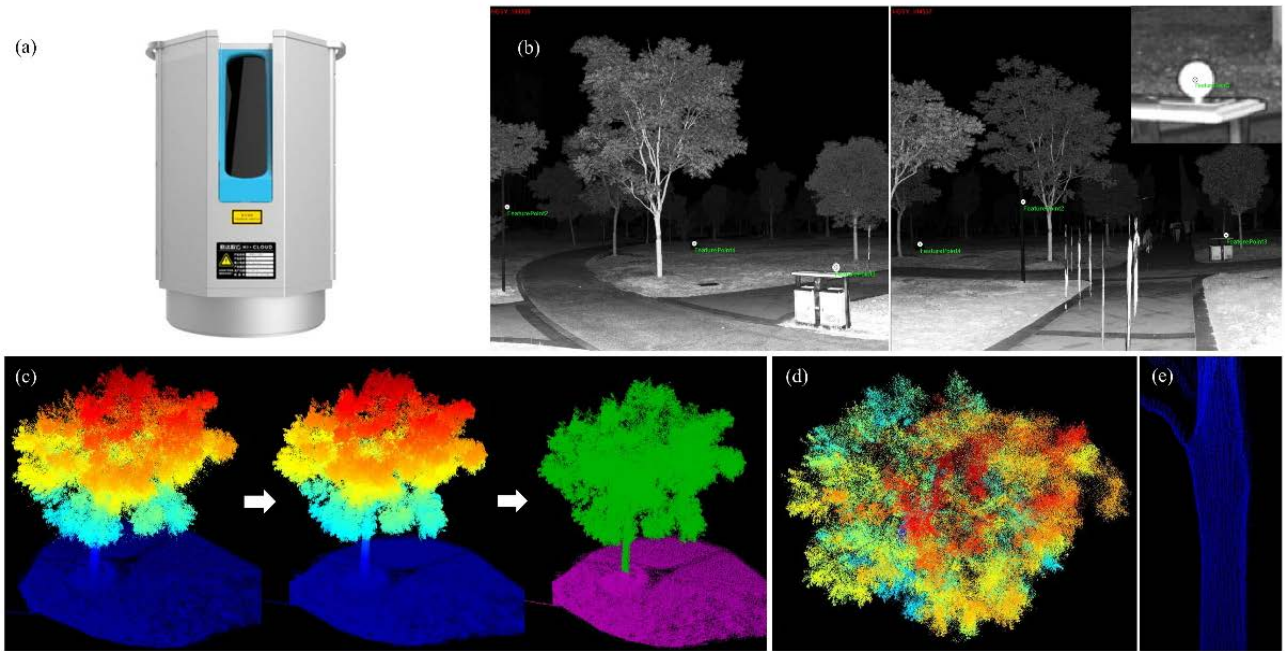

Figure 1. TLS point cloud data acquisition and preprocessing (taking *Sapindus mukorossi* as an example). (a) HS450 model TLS equipment appearance. (b) By marking the target balls of each station to construct the corresponding relationship of the corresponding points, the ICP registration algorithm is used to complete the precise splicing of the point cloud. (c) There are noise points in the original point cloud data, and the number of noise point clouds will be reduced after filtering; ground point recognition clearly divides the single tree and the ground, and completely extracts the single tree point cloud. (d) Canopy top view, which can be used to extract the crown. (e) The longitudinal section of the trunk, showing the details of the trunk.

Generally, pairwise stitching requires at least three homonymous points, that is, the field of view of each station contains at least three target balls.

Point cloud filtering is a key measure to improve the quality of point cloud data processing in the later stage. We limit the goal of filtering to removing discrete point clouds that do not belong to or are easily confused with the target point cloud to eliminate external factors (such as light, personnel movement, etc.) or the noise generated by the instrument itself. Based on KD-tree principle, this paper calculates the Euclidean distance between adjacent point clouds in three-dimensional space, and identifies and eliminates outliers by setting the nearest point number and threshold (usually the threshold is the standard deviation of the average distance from all points to adjacent points) [29].

Point cloud segmentation, that is, the pre-processed single tree point cloud is completely extracted from the root of the trunk to the tip of the tree. The main tasks include selecting the single tree site range and removing the ground point cloud. Due to the small amount of occlusion around each individual tree in this experiment, it is possible to manually select the box along the outer edge of the crown directly under the top view, while the ground point cloud can be identified using a simple morphological filter (SMRF) [30].

The structural parameters of DBH, crown width, tree height and first branch height of TLS single tree point cloud were measured in HDScene software. The canopy volume is obtained with self-compiled function in Matlab Software.

2.3. LAI Branch-Leaf Separation Voxel Model Theory

In indirect measurement of LAI, Beer-Lambert law is the core theoretical basis, which is used to describe the attenuation law of light radiation through uniform medium. However, the plant canopy is not a homogeneous medium, and the distribution of leaves also shows certain aggregation characteristics, which cannot meet the hypothesis of this law. Since then, considering the non-random distribution of canopy leaves [31], Chen and Black *et al.* constructed a classical model of canopy porosity and LAI that has been used so far, as shown in Equation (1):

$$\mathrm{LAI} = \left[-\cos\theta \cdot \ln P(\theta)\right] / G(\theta)\Omega \tag{1}$$

where P is the canopy porosity, θ is the given incident light zenith angle, G is the extinction coefficient and Ω is the aggregation index.

Although the classical LAI model takes into account the aggregation effect, it cannot distinguish the non-photosynthetic wood components such as leaves and branches. At the same time, the traditional optical instruments also have limitations in the separation of branches and leaves, resulting in the estimated LAI values usually contain wood components such as branches, further causing confusion between the measured LAI and its definition [32]. In contrast, the TLS point cloud data has the three-dimensional structural characteristics of individual trees, and there is obvious spatial separation between leaf clusters and branches, which provides data support for branch-leaf separation.

LeWos is a general automatic unsupervised point cloud segmentation algorithm developed by Wang *et al.*, which only needs to pre-set a verticality (*i.e.*, the absolute value of the Z-axis component of the normal vector) threshold between 0.1 and 0.2 to complete branch and leaf separation [33]. The core of the algorithm is based on the search of the point cloud network graph component connection. The point cloud density and the verticality information of the point are added to the graph component construction, and then the point cloud connection node is recursively iterated, and the spatial connection points with similar characteristics are divided into branch clusters or leaf clusters.

A voxel is a cube with the smallest volume size in a three-dimensional model, and its concept is similar to the pixels that make up a two-dimensional image. The voxelization process of point cloud data first needs to set the voxel size (Δx, Δy, Δz) according to the range and resolution of TLS acquisition. At this time, the single-tree point cloud will be stored in the corresponding voxel as many as possible, and then the LAD at each height can be obtained by calculating the beam interception probability. Finally, the LAD of each layer is accumulated along the Z-axis direction to obtain LAI (denoted as $\mathrm{LAI}_{\mathrm{TLS}}$) as shown in **Figure 2**. When using this method, the voxel containing the point cloud can be set to indicate that the light cannot be penetrated, and the corresponding voxel is encoded as 1; the direct transmission of voxel light without point cloud is encoded as 0. Refer to the LAI expression proposed by Hosoi and Omasa based on voxel

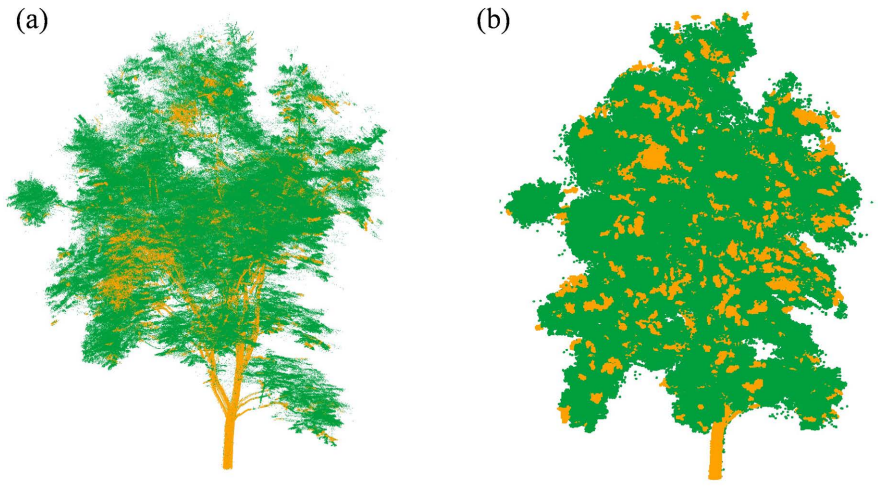

Figure 2. Leaf separation and point cloud voxelization (taking *Koelreuteria paniculata* as an example). (a) LeWos algorithm realizes branch and leaf separation of TLS point cloud data. (b) When the voxel size is 0.0288 m, the point cloud is stored in the voxel.

method [25] (Equation (2)). Since the verification data of Equation (2) are derived from small shrubs, the comprehensive influence of branches is small, and the branches of large trees observed in this experiment have a large occlusion of light. Therefore, we propose a LAI calculation model based on branch-leaf separation point cloud data (Equation (3)).

$$\mathrm{LAI} \cong 1.1 \times \sum_{k=1}^{h} n_1 \Big/ \left(n_1 + n_0\right) \tag{2}$$

$$\mathrm{LAI} \cong 1.1 \times \sum_{k=1}^{h} n_{\mathrm{leaf}} \Big/ \left(n_{\mathrm{leaf}} + n_{\mathrm{empty}} + n_{\mathrm{wood}}\right) \tag{3}$$

where h is the tree height, k is the k-th layer tree height segmentation, n_1 and n_0 are the number of voxels of the k-th layer height encoded as 1 or 0 respectively, n_{leaf}, n_{empty} and n_{wood} are the number of voxels included in the k-th layer height leaf point cloud, no point cloud and branch point cloud respectively, 1.1 is the correction coefficient of the leaf angle when the incident light zenith angle is set to 57.5˚.

2.4. Single Tree Structure Parameters and LAI Verification Data Acquisition

The structural parameters of individual trees include DBH, crown width, tree height and first branch height. The DBH tape, fiber tape and ultrasonic altimeter were used for manual field measurement. The measurement results were used as the real values to evaluate the extraction accuracy of TLS structural parameters of individual trees, and provide basic data for analyzing the relationship between structural parameters of individual trees and LAI.

Because this experiment cannot directly obtain the real LAI through the full harvest method, the LAI-2200 canopy analyzer was used to indirectly obtain the LAI verification data (recorded as LAI_{2200}). The LAI-2200 canopy analyzer is composed of a host and an optical sensor stick. The optical sensor is a convex

"fisheye" lens with a viewing angle of 148˚, which can measure the light intensity changes of the upper and lower canopy at five different zenith angles (7˚, 23˚, 38˚, 53˚, 68˚). The annular detector located inside the lens can send the light intensity attenuation values of five zenith directions to the host, and then derive LAI through the built-in canopy radiation transmission model. In order to meet the observation conditions of heterogeneous tree canopy, it is necessary to choose a cloudy day with stable weather conditions or a sunny morning and evening period that avoids direct light exposure. In addition, interference factors such as shadow and trunk occlusion need to be avoided during measurement. Therefore, this experiment uses 90˚ and 180˚ cover caps to segment the observation area to reduce interference. In the actual operation, the light intensity values corresponding to the upper and lower parts of the canopy were recorded according to the angle of the cover cap around the single tree level for one week, as shown in Figure 3.

2.5. Data Analysis and Model Evaluation

The accuracy of TLS extraction of individual tree structure parameters can be quantitatively evaluated by root mean square error (RMSE). The smaller RMSE indicates the higher accuracy. Pearson correlation coefficient and significance test were used to analyze the linear correlation between individual tree structure parameters and LAI, and to determine the rationality of LAI estimation by voxel model. The calculation formulas of RMSE and correlation coefficient are shown in formulas (4)-(5).

$$\mathrm{RMSE} = \sqrt{\sum_{i=1}^{n}\left(x_i - y_i\right)^2 / n} \tag{4}$$

$$r = \frac{\sum_{i=1}^{n}\left(x_i - \overline{x}\right)\left(y_i - \overline{y}\right)}{\sqrt{\sum_{i=1}^{n}\left(x_i - \overline{x}\right)^2}\sqrt{\sum_{i=1}^{n}\left(y_i - \overline{y}\right)^2}} \tag{5}$$

where $y_{i,j}$ is the i-th and j-th measured values, $x_{i,j}$ is the i-th and j-th TLS extracted values, $\overline{x}, \overline{y}$ are the mean values of the two, respectively, and n is the sample size.

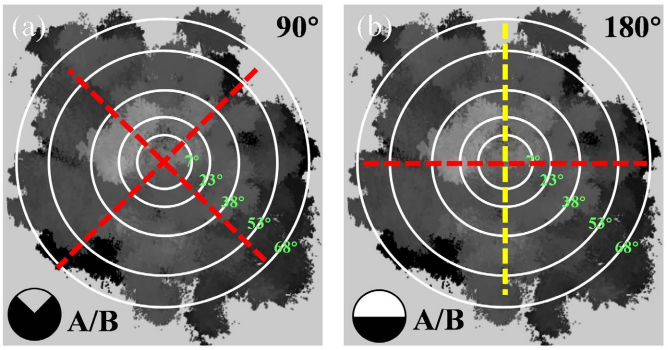

Figure 3. Measurement of LAI-2200 canopy analyzer. (a) Select 90˚ cover cap, according to the order of ABBBBABBBBA, repeat three times. (b) 180˚ cover cap, measured in ABBABBA order, repeated three times. The A value represents the light intensity of the upper canopy, and the B value represents the light intensity of the lower canopy.

3. Results and Analysis

3.1. Accuracy Analysis of Single Wood Structure Parameters Extracted by TLS

The DBH, tree height, crown width and first branch height extracted by TLS were compared with the results of manual measurement to quantitatively evaluate the instrument measurement accuracy of TLS. The results are shown in Figure 4. It can be seen that there is a good linear relationship between the DBH, tree height, crown width and the first branch height extracted by TLS and the corresponding measured values, and the scatter points are roughly distributed near the 1:1 straight line. Among them, the RMSE value of the DBH extraction error is only 0.3087 cm, and the overall distribution of the scatter plot has no obvious high and low deviation tendency, which indicates that the trunk point cloud can accurately record the dry contour details. The extraction errors of tree height and crown width were also maintained at a low level as a whole, and the RMSE values were 0.3723 m and 0.3306 m, respectively, which further indicated that the single tree 3D model of TLS and the real tree also maintained good

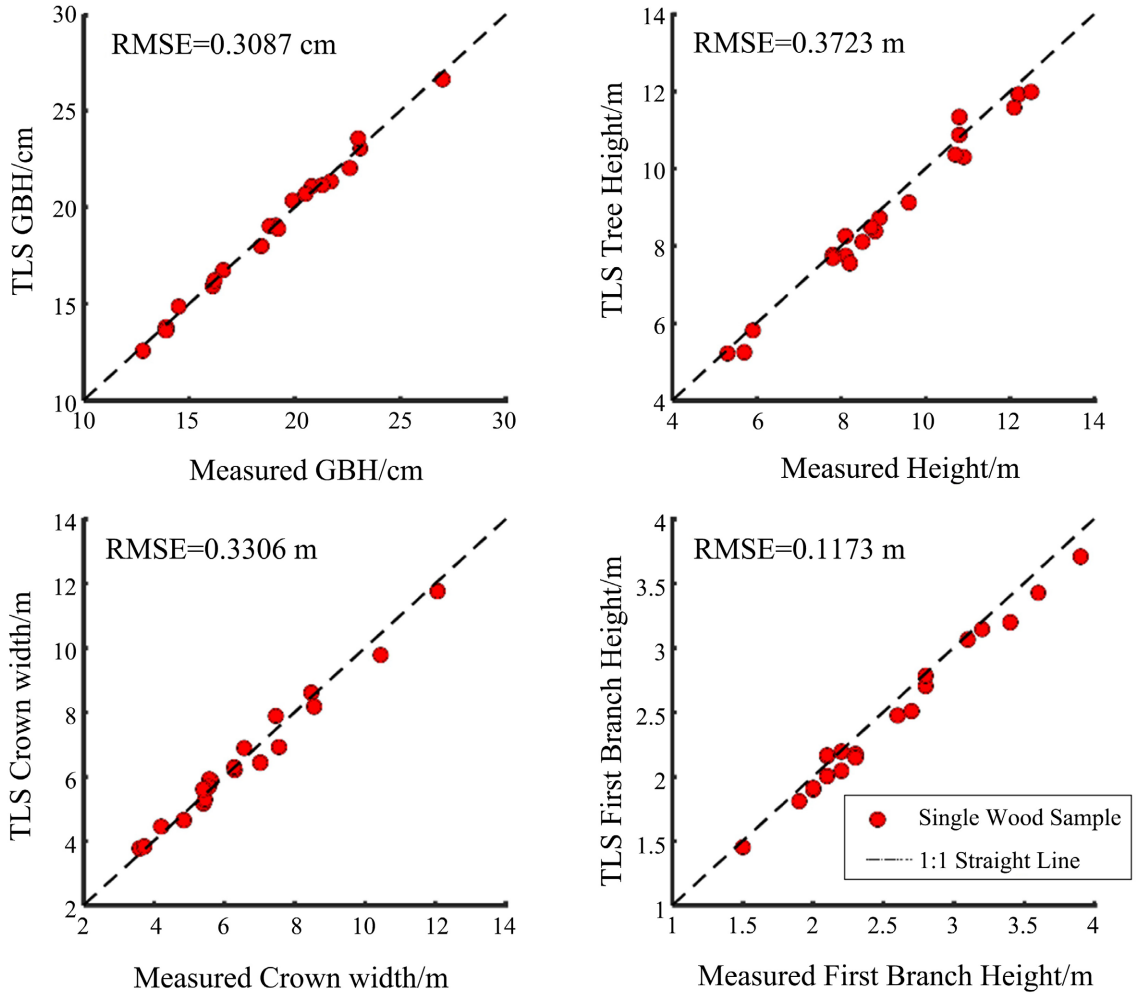

Figure 4. Scatter plot of extracted and measured values of four TLS single wood structure parameters.

consistency at the vertical height and crown width levels. By observing the scatter distribution of the first branch, it is found that there is a certain degree of underestimation deviation between the TLS extraction value and the measured value. This error may come from the difference in the interpretation of the surveyor at the critical position of the first branch. In general, the TLS extraction errors of the four single-tree structural parameters all meet the needs of real-world conversion, and the characteristics of trunks, branches and leaves of trees retain good authenticity. Therefore, we can directly use TLS data to estimate the real LAI.

3.2. Correlation Analysis between LAI_{TLS} and LAI_{2200} with Different Voxel Sizes

Based on the point cloud resolution (0.0288 m) set by the instrument during TLS measurement, eight gradients of voxel size non-equidistant setting 0.01 m, 0.03 m, 0.05 m, 0.1 m, 0.15 m, 0.3 m, 0.6 m, 1.2 m were used to estimate the LAI_{TLS} of removing woody components, and the correlation analysis was performed with the LAI_{2200} measured by the canopy analyzer under the 90˚ and 180˚ cover caps, respectively (Figure 5). It can be seen from Figure 5 that there is a significant positive linear correlation between 90˚ LAI and 180˚ LAI observed by LAI-2200

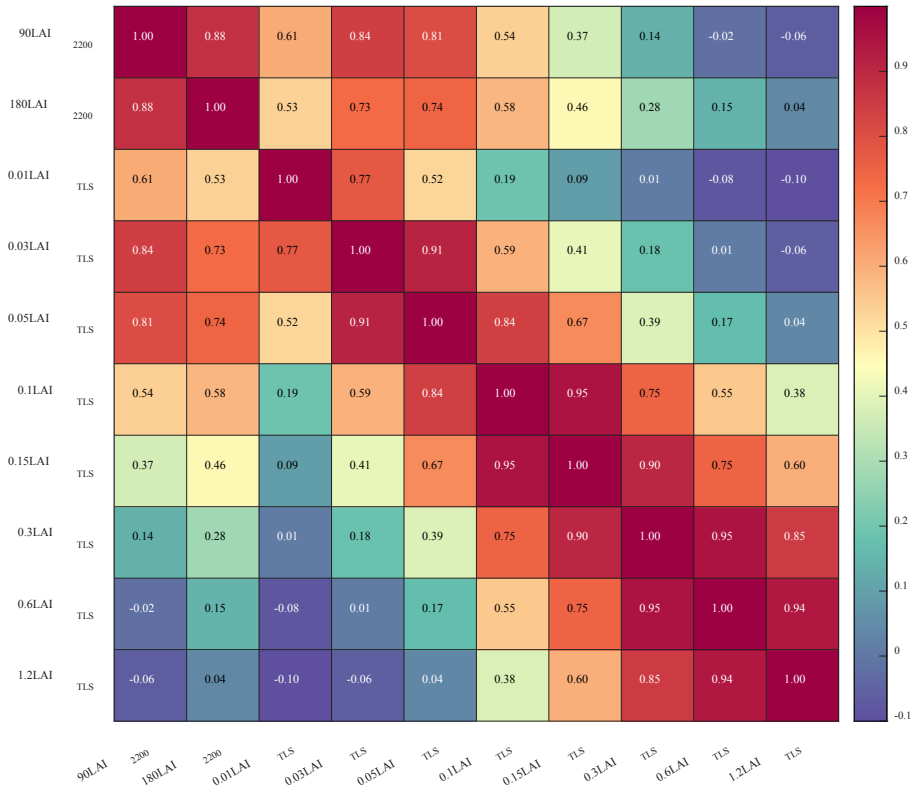

Figure 5. Correlation coefficient heat map of LAI_{TLS} and LAI_{2200} with different voxel sizes. Note: * indicates that there is a correlation between the two quantitative data. At this time, the correlation coefficient is meaningful. * indicates that the correlation is significant at the 0.05 level test, and * * indicates that the correlation is significant at the 0.01 level test.

canopy analyzer, and the correlation coefficient $r = 0.88$, indicating that there are differences in the observation of the same target using different angle masks, but the overall trend is still consistent. Obviously, from the results of different voxel sizes, the closer the set voxel size is to the point cloud resolution, the more significant the correlation with LAI_{2200}. Among them, when the voxel size was set at 0.01 m - 0.1 m, the correlation with LAI_{2200} measured under 90˚ and 180˚ caps reached a very significant level, and the 0.03 m voxel size had higher correlation coefficients under the same reference ($r = 0.84$ and 0.73). When the voxel size is set more than 0.1 m, the correlation coefficient with the LAI_{2200} measured under the 90˚ and 180˚ cover caps gradually decreases. When the voxel size exceeds 0.3 m, the linear correlation between them is basically not significant. This shows that the reasonable setting of voxel size is very important for the calculation of the true value of LAI. In addition, the correlation coefficient between the LAI_{2200} of the 180˚ canopy cover and the LAI estimated by the voxel method is lower than that of the 90˚ canopy cover. The reason may be related to the number of observations of the B value of the different angle canopy cover. The number of B values required for the observation of the 90˚ canopy cover can capture the attenuation information of the light intensity in all directions of the canopy. Therefore, the 90˚ canopy cover has higher measurement accuracy.

We draw a box plot (**Figure 6**) based on the data distribution differences between LAI_{TLS} and LAI_{2200} with different voxel sizes, and observe the range of LAI values estimated by the voxel model after the separation of branch and leaf point clouds. It can be seen from the figure that the LAI_{TLS} value increases first and then decreases with the gradient change. Among them, although the LAI_{TLS} close to the point cloud resolution voxel size has a similar trend to the measured value LAI_{2200}, the LAI value is generally greater than the measured value of the canopy analyzer. At the same time, we found that the overall change of LAI value from 0.03 m to 0.01 m was much larger than that from 0.03 m to 1.2 m, that is, the smaller the voxel size, the more severe the decrease trend of LAI value. On the whole, LAI_{2200} is basically in the low value estimation interval compared with LAI_{TLS}. Combined with the common underestimation phenomenon of canopy analyzer, TLS shows the advantage of easily breaking through the limitation of LAI observation underestimation.

3.3. Correlation Analysis between LAI and Structural Parameters of Single Tree

The LAI_{TLS} of LAI_{2200} and 0.03 m voxel size were correlated with individual tree structure parameters (DBH, tree height, crown width, first branch height and canopy volume) (**Figure 7**). It can be seen that LAI_{2200} and LAI_{TLS} were significantly negatively correlated with crown width, and the correlation coefficients with DBH, tree height, first branch height and canopy volume were negative. This indicates that the more compact the horizontal and vertical structure of trees, the larger the ratio of leaf area to ground projection. Explained by definition, in the case of the same number of leaves, the shrinkage of the horizontal

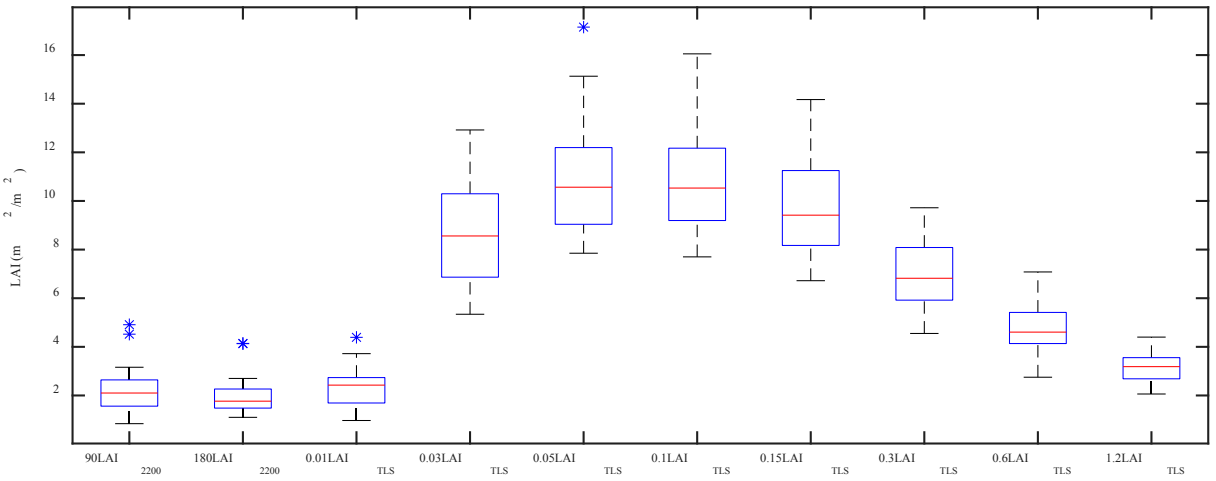

Figure 6. Numerical distribution box plots of LAI_{TLS} and LAI_{2200} with different voxel sizes.

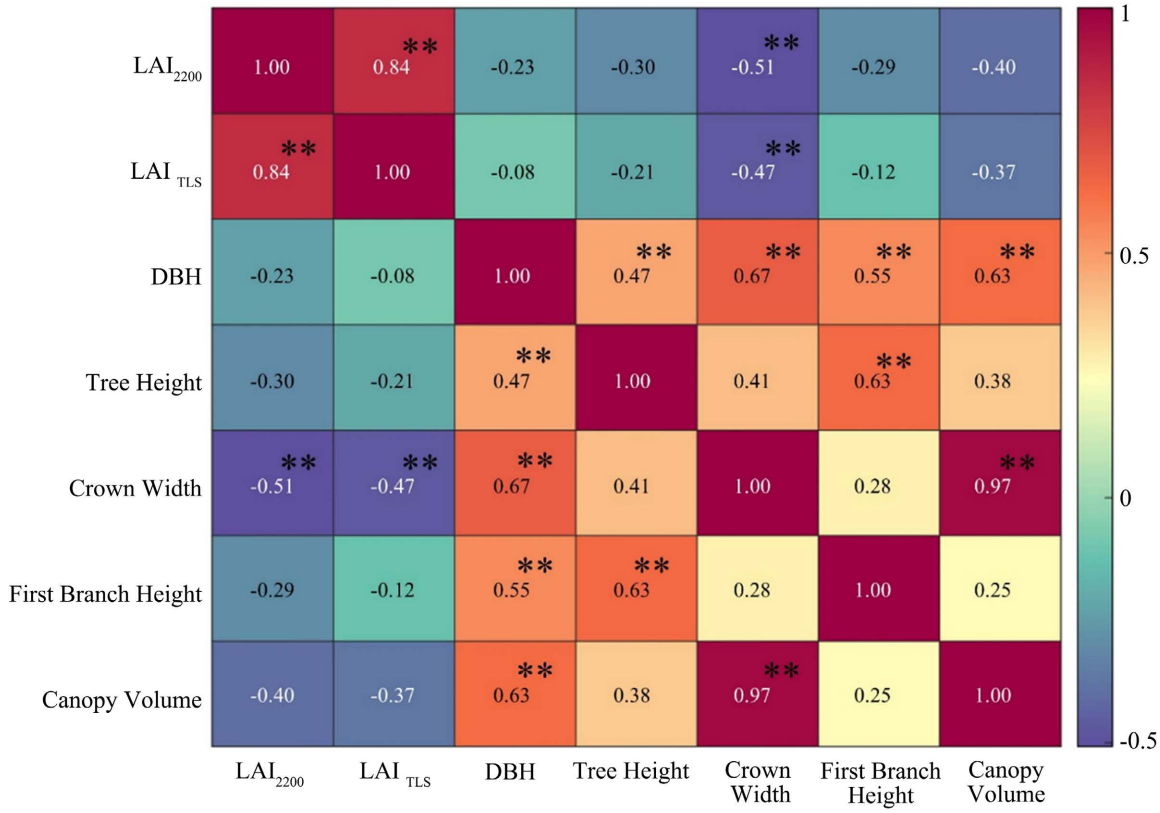

Figure 7. Heatmaps of correlation coefficients between LAI_{2200} and LAI_{TLS} with 0.03 m voxel size and individual structural parameters.

structure of a single tree reduces the surface occupied area of the tree, the layered LAD value increases, and the LAI value accumulates. On the other hand, DBH and other single tree structure parameters, crown width and canopy volume showed a significant positive correlation, so the characteristics of tree growth tend to open state. Therefore, with the growth of trees, the LAI value will have a downward trend, which means that the LAI value of trees is not the larger

the higher the ecological benefits, but is closely related to the growth status of trees.

4. Discussion

The point cloud data of different varieties of trees with high-precision vertical and horizontal depth information were obtained by TLS. On the basis of branch and leaf separation, the LAI estimation model was modified by voxel method, and the correlation between LAI estimation values of different voxel sizes and the measured values of LAI-2200 canopy analyzer was compared. The results theoretical model of this study is feasible in LAI estimation.

This study found that voxel size directly affects the accuracy of LAI estimation. The larger the voxel setting, the larger the number of point clouds per unit voxel content, and the overall LAD of each height layer showed a trend of increasing first and then decreasing, which in turn affected the overall estimation interval of LAI. We observed that when the voxel size is close to the minimum point cloud spacing set by the TLS instrument, it has a strong correlation with the measured value of the canopy analyzer, which is consistent with the conclusion that Li *et al.* [34] [35] used the average distance between point cloud data as the voxel size to estimate LAI more accurately. The spatial distribution of point cloud distance is expressed as point cloud density, and the point cloud density is different at different heights or distances because the instrument measurement parameters are fixed. Therefore, we fix the global voxel size with a uniform value of the average distance, which does not reflect the change of density of point cloud data at different positions of trees. Leila *et al.* proposed an adaptive voxelization strategy based on the variable local spatial point cloud density and the natural characteristics of the canopy, which effectively reduced the calculation error of LAI intermediate auxiliary parameters (such as porosity) [36]. This provides a research idea for the subsequent optimization of voxel adaptation size according to the point cloud density at different positions of a single tree.

Due to the limitations of traditional optical sensor instruments, LAI estimates often include wood components and cannot reflect the true LAI of leaves. [37] Based on the characteristics of TLS data, LeWos algorithm is used to identify and eliminate branches, which can effectively remove the influence of wood components and then estimate the real LAI. The LeWos unsupervised algorithm in this paper can basically obtain better branch and leaf separation effect, but in the natural state, the mutual occlusion of branches and leaves will lead to the loss of some internal information and cannot separate the complete branches or leaves. At the same time, the vertical detection depth of TLS on the ground is limited, and the point cloud information of the upper canopy of tall trees will still be lost. However, the lack of point cloud information is a thorny problem. It is necessary to establish a tree digital point cloud sample library by multi-angle and multi-position laser scanning to obtain a more abundant single-tree model, and

train appropriate machine learning algorithms to fill in the missing parts according to the structural characteristics [38]. At present, due to the large workload and high cost of data acquisition, related research needs to be further studied.

In this study, although a modified model of voxel LAI estimation based on branch and leaf separation algorithm was proposed, this method was only indirectly verified by LAI-2200 canopy analyzer, which could not be compared with the real LAI of trees. In the next step, a small number of small shrubs or low trees were selected and directly verified by the whole harvest method. In the future research, we can also consider the recognition of leaf point cloud and the reconstruction of leaf components, and directly calculate the surface area of all leaves to obtain a more realistic LAI, which will truly break through from the definition level. This will also be an important way to indirectly measure many theories, in addition to considering factors such as leaf aggregation effect, zenith angle, leaf inclination distribution, and non-photosynthetic components [39]. With the deepening of research technology, the high-fidelity characteristics of TLS point cloud data will provide key support for mining more deep information of LAI.

5. Conclusions

In this paper, the three-dimensional point cloud data of 20 trees were obtained by TLS technology, and the point cloud voxelization method was combined with LeWos algorithm to propose a single tree canopy LAI estimation model for removing the woody components of branches and branches. Then, the difference between the eight voxel sizes of 0.01 m, 0.03 m, 0.05 m, 0.1 m, 0.15 m, 0.3 m, 0.6 m and 1.2 m and the observed values of LAI-2200 canopy analyzer was explored. The following conclusions were obtained:

1) TLS provides accurate horizontal and vertical structure information of different tree species. The structural parameters of DBH, crown width, tree height and first branch height extracted by TLS have very low relative error with manual measurement results, which fully meets the high fidelity and high precision acquisition of three-dimensional spatial structure characteristics of trees.

2) The closer the voxel size is to the point cloud resolution set during TLS acquisition, the stronger the correlation between the point cloud resolution and the indirect measurement results of the canopy analyzer. At the same time, as the voxel size changes before and after the point cloud resolution, the LAI estimation value generally shows a trend of increasing first and then decreasing.

3) The LAI values calculated by canopy analyzer and TLS were consistent with the single tree structure parameters, which showed that the compact tree structure often had a larger LAI value.

In this paper, TLS point cloud is used as the direct data source, which effectively avoids the limitations of the two-dimensional geographic projection method, and comprehensively considers the factors of voxel size and wood compo-

sition, and provides a way to estimate the high-precision LAI values of different tree species.

Conflicts of Interest

The authors declare no conflicts of interest regarding the publication of this paper.

References

[1] Niinemets, U., Keenan, T.F. and Hallik, L. (2015) A Worldwide Analysis of Within-Canopy Variations in Leaf Structural, Chemical and Physiological Traits across Plant Functional Types. *New Phytologist*, **205**, 973-993. https://doi.org/10.1111/nph.13096

[2] Majasalmi, T. and Rautiainen, M. (2020) The Impact of Tree Canopy Structure on Understory Variation in a Boreal Forest. *Forest Ecology and Management*, **466**, Article ID: 118100. https://doi.org/10.1016/j.foreco.2020.118100

[3] Gough, C.M., Atkins, J.W., Fahey, R.T. and Hardiman, B.S. (2019) High Rates of Primary Production in Structurally Complex Forests. *Ecology*, **100**, e02864. https://doi.org/10.1002/ecy.2864

[4] Ehbrecht, M., Schall, P., Ammer, C., Fischer, M. and Seidel, D. (2019) Effects of Structural Heterogeneity on the Diurnal Temperature Range in Temperate Forest Ecosystems. *Forest Ecology and Management*, **432**, 860-867. https://doi.org/10.1016/j.foreco.2018.10.008

[5] Xu, J., Quackenbush, L.J., Volk, T.A. and Im, J. (2020) Forest and Crop Leaf Area Index Estimation Using Remote Sensing: Research Trends and Future Directions. *Remote Sensing*, **12**, Article No. 2934. https://doi.org/10.3390/rs12182934

[6] Breda, N.J.J. (2003) Ground-Based Measurements of Leaf Area Index: A Review of Methods, Instruments and Current Controversies. *Journal of Experimental Botany*, **54**, 2403-2417. https://doi.org/10.1093/jxb/erg263

[7] Chen, J.-M. and Black, T.A. (1992) Defining Leaf Area Index for Non-Flat Leaves. *Plant, Cell and Environment*, **15**, 421-429. https://doi.org/10.1111/j.1365-3040.1992.tb00992.x

[8] Macfarlane, C., Hoffman, M., Eamus, D., Kerp, N., Higginson, S., McMurtrie, R. and Adams, M. (2007) Estimation of Leaf Area Index in Eucalypt Forest Using Digital Photography. *Agricultural and Forest Meteorology*, **143**, 176-188. https://doi.org/10.1016/j.agrformet.2006.10.013

[9] Wei, S.-S., Yin, T.-G., Dissegna, M.A., Whittle, A.J., Ow, G.L.F., *et al.* (2020) An Assessment Study of Three Indirect Methods for Estimating Leaf Area Density and Leaf Area Index of Individual Trees. *Agricultural and Forest Meteorology*, **292**, Article ID: 108101. https://doi.org/10.1016/j.agrformet.2020.108101

[10] Tan, C.-W., Zhang, P.-P., Zhou, X.-X., *et al.* (2020) Quantitative Monitoring of Leaf Area Index in Wheat of Different Plant Types by Integrating NDVI and Beer-Lambert Law. *Scientific Reports*, **10**, Article No. 929. https://doi.org/10.1038/s41598-020-57750-z

[11] Brown, L.A., Ogutu, B.O. and Dash, J. (2020) Tracking Forest Biophysical Properties with Automated Digital Repeat Photography: A Fisheye Perspective Using Digital Hemispherical Photography from below the Canopy. *Agricultural and Forest Meteorology*, **287**, Article ID: 107944.

https://doi.org/10.1016/j.agrformet.2020.107944

[12] Qu, Y.-H., Wang, Z.-X., Shang, J.-L., Liu, J.-G. and Zou, J. (2021) Estimation of Leaf Area Index Using Inclined Smartphone Camera. *Computers and Electronics in Agriculture*, **191**, Article ID: 106514. https://doi.org/10.1016/j.compag.2021.106514

[13] Jonckheere, I., Fleck, S., Nackaerts, K., *et al.* (2004) Review of Methods for *in Situ* Leaf Area Index Determination—Part I. Theories, Sensors and Hemispherical Photography. *Agricultural and Forest Meteorology*, **121**, 19-35. https://doi.org/10.1016/j.agrformet.2003.08.027

[14] Yan, G.-J., Hu, R.-H., Luo, J.-H., *et al.* (2019) Review of Indirect Optical Measurements of Leaf Area Index: Recent Advances, Challenges, and Perspectives. *Agricultural and Forest Meteorology*, **265**, 390-411. https://doi.org/10.1016/j.agrformet.2018.11.033

[15] Srinet, R., Nandy, S. and Patel, N.R. (2019) Estimating Leaf Area Index and Light Extinction Coefficient Using Random Forest Regression Algorithm in a Tropical Moist Deciduous Forest, India. *Ecological Informatics*, **52**, 94-102. https://doi.org/10.1016/j.ecoinf.2019.05.008

[16] Liu, J., Skidmore, A.K., Wang, T.-J., *et al.* (2019) Variation of Leaf Angle Distribution Quantified by Terrestrial LiDAR in Natural European Beech Forest. *ISPRS Journal of Photogrammetry and Remote Sensing*, **148**, 208-220. https://doi.org/10.1016/j.isprsjprs.2019.01.005

[17] Wang, Y. and Fang, H.-L. (2020) Estimation of LAI with the LiDAR Technology: A Review. *Remote Sensing*, **12**, Article No. 3457. https://doi.org/10.3390/rs12203457

[18] Wulder, M.A., White, J.C., Nelson, R.F., *et al.* (2012) Lidar Sampling for Large-Area Forest Characterization: A Review. *Remote Sensing of Environment*, **121**, 196-209. https://doi.org/10.1016/j.rse.2012.02.001

[19] Camarretta, N., Harrison, P.A., Bailey, T., *et al.* (2020) Monitoring Forest Structure to Guide Adaptive Management of Forest Restoration: A Review of Remote Sensing Approaches. *New Forests*, **51**, 573-596. https://doi.org/10.1007/s11056-019-09754-5

[20] Sumnall, M.J., Albaugh, T.J., Carter, D.R., *et al.* (2022) Effect of Varied Unmanned Aerial vehicle Laser Scanning Pulse Density on Accurately Quantifying Forest Structure. *International Journal of Remote Sensing*, **43**, 721-750. https://doi.org/10.1080/01431161.2021.2023229

[21] Vincent, G., Antin, C., Laurans, M., *et al.* (2017) Mapping Plant Area Index of Tropical Evergreen Forest by Airborne Laser Scanning. A Cross-Validation Study Using LAI_{2200} Optical Sensor. *Remote Sensing of Environment*, **198**, 254-266. https://doi.org/10.1016/j.rse.2017.05.034

[22] Korhonen, L., *et al.* (2017) Comparison of Sentinel-2 and Landsat 8 in the Estimation of Boreal Forest Canopy Cover and Leaf Area Index. *Remote Sensing of Environment*, **195**, 259-274. https://doi.org/10.1016/j.rse.2017.03.021

[23] Calders, K., Adams, J., Armston, J., *et al.* (2020) Terrestrial Laser Scanning in Forest Ecology: Expanding the Horizon. *Remote Sensing of Environment*, **251**, Article ID: 112102. https://doi.org/10.1016/j.rse.2020.112102

[24] Zheng, G., Moskal, L.M. and Kim, S.H. (2013) Retrieval of Effective Leaf Area Index in Heterogeneous Forests with Terrestrial Laser Scanning. *IEEE Transactions on Geoscience and Remote Sensing*, **51**, 777-786. https://doi.org/10.1109/TGRS.2012.2205003

[25] Hosoi, F. and Omasa, K. (2006) Voxel-Based 3-D Modeling of Individual Trees for Estimating Leaf Area Density Using High-Resolution Portable Scanning Lidar. *IEEE*

Transactions on Geoscience and Remote Sensing, **44**, 3610-3618. https://doi.org/10.1109/TGRS.2006.881743

[26] Olsoy, P.J., Glenn, N.F., Clark, P.E. and Derryberry, D.R. (2014) Aboveground Total and Green Biomass of Dryland Shrub Derived from Terrestrial Laser Scanning. *ISPRS Journal of Photogrammetry and Remote Sensing*, **88**, 166-173. https://doi.org/10.1016/j.isprsjprs.2013.12.006

[27] Li, W., Niu, Z., Huang, N., *et al.* (2015) Airborne LiDAR Technique for Estimating Biomass Components of Maize: A Case Study in Zhangye City, Northwest China. *Ecological Indicators*, **57**, 486-496. https://doi.org/10.1016/j.ecolind.2015.04.016

[28] Gressin, A., Mallet, C., Demantke, J. and David, N. (2013) Towards 3D Lidar Point Cloud Registration Improvement Using Optimal Neighborhood Knowledge. *ISPRS Journal of Photogrammetry and Remote Sensing*, **79**, 240-251. https://doi.org/10.1016/j.isprsjprs.2013.02.019

[29] Li, Y.-Y., Wang, J., Li, B., Sun, W.-X. and Li, Y.-Y. (2021) An Adaptive Filtering Algorithm of Multilevel Resolution Point Cloud. *Survey Review*, **53**, 300-311. https://doi.org/10.1080/00396265.2020.1755163

[30] Pingel, T.J., Clarke, K.C. and McBride, W.A. (2013) An Improved Simple Morphological Filter for the Terrain Classification of Airborne LIDAR Data. *ISPRS Journal of Photogrammetry and Remote Sensing*, **77**, 21-30. https://doi.org/10.1016/j.isprsjprs.2012.12.002

[31] Chen, J.M. and Black, T.A. (1991) Measuring Leaf Area Index of Plant Canopies with Branch Architecture. *Agricultural and Forest Meteorology*, **57**, 1-12. https://doi.org/10.1016/0168-1923(91)90074-Z

[32] Chen, J.-M. (1996) Optically-Based Methods for Measuring Seasonal Variation of Leaf Area Index in Boreal Conifer Stands. *Agricultural and Forest Meteorology*, **29**, 135-163. https://doi.org/10.4095/218392

[33] Wang, D., Takoudjou, S.M. and Casella, E. (2020) LeWoS: A Universal Leaf-Wood Classification Method to Facilitate the 3D Modelling of Large Tropical Trees Using Terrestrial LiDAR. *Methods in Ecology and Evolution*, **11**, 376-389. https://doi.org/10.1111/2041-210X.13342

[34] Li, S.-H., Dai, L.-Y., Wang, H.-S., *et al.* (2017) Estimating Leaf Area Density of Individual Trees Using the Point Cloud Segmentation of Terrestrial LiDAR Data and a Voxel-Based Model. *Remote Sensing*, **9**, Article No. 1202. https://doi.org/10.3390/rs9111202

[35] Li, Y.-M., Guo, Q.-H., Tao, S.-L., *et al.* (2016) Derivation, Validation, and Sensitivity Analysis of Terrestrial Laser Scanning-Based Leaf Area Index. *Canadian Journal of Remote Sensing*, **42**, 719-729. https://doi.org/10.1080/07038992.2016.1220829

[36] Taheriazad, L., Moghadas, H. and Sanchez-Azofeifa, A. (2019) Calculation of Leaf Area Index in a Canadian Boreal Forest Using Adaptive Voxelization and Terrestrial LiDAR. *International Journal of Applied Earth Observation and Geoinformation*, **83**, Article ID: 101923. https://doi.org/10.1016/j.jag.2019.101923

[37] Wang, D., Brunner, J., Ma, Z.-Y., *et al.* (2018) Separating Tree Photosynthetic and Non-Photosynthetic Components from Point Cloud Data Using Dynamic Segment Merging. *Forests*, **9**, Article No. 252. https://doi.org/10.3390/f9050252

[38] Zhu, X., Liu, J., Skidmore, A.K., *et al.* (2020) A Voxel Matching Method for Effective Leaf Area Index Estimation in Temperate Deciduous Forests from Leaf-On and Leaf-Off Airborne LiDAR Data. *Remote Sensing of Environment*, **240**, Article ID: 111696. https://doi.org/10.1016/j.rse.2020.111696

[39] Parker, G.G. (2020) Tamm Review: Leaf Area Index (LAI) Is both a Determinant and a Consequence of Important Processes in Vegetation Canopies. *Forest Ecology and Management*, **477**, Article ID: 118496. https://doi.org/10.1016/j.foreco.2020.118496